

## In-situ investigation of the order-disorder transition in $\text{Cu}_2\text{ZnSnSe}_4$ by optical transmission spectroscopy

Christiane Stroth,<sup>1</sup> Mohamed H. Sayed,<sup>1</sup> Janet Neerken,<sup>1</sup> Ulf Mikolajczak,<sup>1</sup> Germain Rey,<sup>2</sup> Jürgen Parisi,<sup>1</sup> and Levent Gütaý<sup>1,a</sup>

<sup>1</sup>Laboratory for Chalcogenide Photovoltaics, Energy and Semiconductor Research Laboratory, University of Oldenburg, 26129 Oldenburg, Germany

<sup>2</sup>Laboratory for Photovoltaics, University of Luxembourg, 4422 Belvaux, Luxembourg

(Received 9 September 2016; accepted 27 January 2017; published online 13 February 2017)

The existence of disorder is one possible reason for the limited performance of kesterite solar cells. Therefore further knowledge of the order-disorder phase transition, of factors which influence the degree of order and of methods to determine this material property is still required. In this study we investigated the order-disorder transition in the kesterite material  $\text{Cu}_2\text{ZnSnSe}_4$  by in-situ optical transmission spectroscopy during heat treatments. We show in-situ results for the temperature dependence of the band gap and its tailing properties. The influence of cooling rates on the phase transition was analyzed as well as the ordering kinetics during annealing at a constant temperature. The critical temperature of the phase transition was determined and the existence of a control temperature range is shown, which allows for controlling the degree of order by the cooling rate within this range. Additionally we performed Raman analysis to link Raman spectra to the degree of order in  $\text{Cu}_2\text{ZnSnSe}_4$ . A correlation between the intensity ratio of A-modes as well as B-/E- Raman modes and the degree of order was found. © 2017 Author(s). All article content, except where otherwise noted, is licensed under a Creative Commons Attribution (CC BY) license (<http://creativecommons.org/licenses/by/4.0/>). [<http://dx.doi.org/10.1063/1.4976619>]

For thin film solar cells based on the semiconductor kesterite, best power conversion efficiencies do not exceed 13 % up to now.<sup>1</sup> Recently, disorder in the Cu-Zn planes of the kesterite crystal structure is discussed as a limiting factor for the solar cell performance and as a reason for the observed open circuit voltage ( $V_{oc}$ ) deficit.<sup>2-5</sup> This disorder can be influenced by heat treatments and was detected in powders by neutron diffraction<sup>6</sup> and NMR.<sup>7</sup> Scragg et al.<sup>8</sup> investigated  $\text{Cu}_2\text{ZnSnS}_4$  (CZTS) thin films exposed to different annealing temperatures by Raman spectroscopy and found a critical temperature for the order-disorder phase transition of  $T_c = (260 \pm 10)$  °C. This means, above  $T_c$  the Cu and Zn atoms are distributed randomly on their sites in the  $z = 1/4$  and  $z = 3/4$  planes in the crystal, while below  $T_c$  the degree of order increases with decreasing annealing temperature as well as cooling rate.<sup>9</sup> For  $\text{Cu}_2\text{ZnSnSe}_4$  (CZTSe) thin films Rey et al.<sup>10</sup> showed, that the critical temperature is  $T_c = (200 \pm 20)$  °C. Furthermore, in this study it was shown by applying Vineyard's model,<sup>11</sup> that the band gap  $E_g$  can be used as a secondary order parameter, i.e.  $E_g$  represents the degree of order in CZTSe and increases with increasing order. Töbrens et al.<sup>12</sup> observed the Cu/Zn ordering by anomalous X-ray diffraction and determined the critical temperature for CZTSe at  $(203 \pm 6)$  °C. For CZTSSe samples with an S/Se ratio of approximately 8 % Krämmer et al.<sup>13</sup> studied the kinetics of the order-disorder transition and specified the critical temperature of  $T_c = (195 \pm 5)$  °C by using electroreflectance for determining the band gap of samples after different annealing treatments.

In the present work, we investigated the order-disorder transition in CZTSe thin films by in-situ transmission spectroscopy. This approach allows for recording the phase transition during the annealing procedure by observing the change in the absorption edge at full control of the sample temperature. This allows for extracting band gaps and Urbach energies for the measured temperature range. Furthermore, Raman analysis at room temperature after the heat treatments was performed

<sup>a</sup>Author to whom correspondence should be addressed. Electronic mail: [levent.guetay@uni-oldenburg.de](mailto:levent.guetay@uni-oldenburg.de)



to investigate the relation of the Raman fingerprints with the degree of order in the film, like it was shown for CZTS.<sup>8,9</sup>

The investigated CZTSe sample with composition of  $\text{Cu}/(\text{Zn}+\text{Sn}) \approx 0.8$  and  $\text{Zn}/\text{Sn} \approx 1.2$  was fabricated on a glass substrate by a high temperature co-evaporation process which is described elsewhere.<sup>14</sup> Companion absorbers deposited onto Mo-coated glass substrate and processed to solar cell devices reached solar cell efficiencies in the range of 5 to 7%.<sup>3</sup> The sample was divided into three pieces: one piece remained in an as-prepared state for later reference, another piece was disordered by annealing on a hotplate at 255 °C for two hours in  $\text{N}_2$  atmosphere and rapidly being cooled down to freeze the disorder in the crystal, the third piece was used for the in-situ transmission experiments (in the following the samples are labeled as ‘as-prepared’, ‘disordered’ and ‘in-situ’, respectively).

The in-situ transmission experiments were realized in a home build setup, which consists nominally of a cage like sample holder equipped with a PID controlled ceramic heater. The sample temperature was measured by a Pt100 sensor placed at the surface of the CZTSe layer. A hole of 4 mm diameter in the centre of the sample holder allowed for a perpendicular incidence angle of the transmission measurement. A fiber coupled halogen lamp was used as light source. The transmitted photons were focused into an optical fiber and recorded by a detector system consisting of a spectrometer and a 256-pixel InGaAs detector array. All heat treatments were conducted under  $\text{N}_2$  atmosphere. Four experiments with different cooling rates were performed. In each run the sample ‘in-situ’ was first heated up to a temperature  $> 270$  °C, which is far above the critical temperature  $T_c = (200 \pm 20)$  °C reported earlier,<sup>10</sup> followed by a cooling process with different cooling rates of 0.5 °C/min, 1.3 °C/min, 6.5 °C/min and an uncontrolled natural cooling, realized by turning off the heater, which is the maximal cooling rate applied in this experiment. For this case the cooling rate is not constant and amounts to  $\approx 20$  °C/min for the relevant temperature range of 210 to 140 °C, which will be discussed later.

Transmission spectra were recorded every 2 s for the 0.5 °C/min rate and every 1 s for all other cooling rates. For a further investigation of the kinetics of the ordering in CZTSe, the ‘in-situ’ sample was first disordered as explained before. Thereafter the sample was heated up to  $(122 \pm 5)$  °C and kept at this temperature for approximately 15 h, recording a transmission spectrum every 5 s. For comparison room temperature transmission measurements were done on the samples ‘disordered’ and ‘as-prepared’.

Additionally Raman spectra were recorded at room temperature in a Horiba LabRAM Aramis microscope with an excitation wavelength of 532 nm, an excitation laser power of 3 mW and a laser spot size of approximately 1  $\mu\text{m}$  for all samples after each heat treatment.

Figure 1(a) shows exemplarily selected transmission spectra of the ‘in-situ’ sample recorded in a temperature range between 270 °C and 30 °C while cooling down with a rate of 0.5 °C/min. It can be clearly seen that the absorption edge shifts to higher photon energies with decreasing temperature. This expected behavior can be explained by two simultaneous effects: (i) below the critical temperature  $T_c$  the band gap is influenced by the phase transition from disordered to ordered CZTSe and (ii) the band gaps of semiconductors depend on the temperature due to electron-phonon interaction

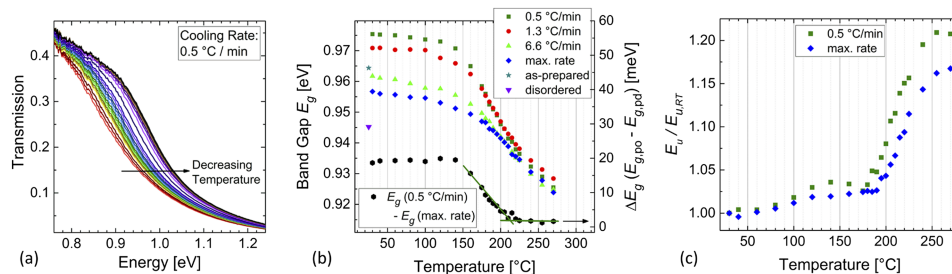


FIG. 1. (a) In-situ transmission spectra showing the shifting absorption edge during cool down at a rate of 0.5 °C/min; (b) band gap energy development for cooling down at different cooling rates, and  $\Delta E_g (E_{g,po} - E_{g,pd})$  calculated from the results of the most preferentially ordered ( $E_{g,po}$  from 0.5 °C/min) and most preferentially disordered ( $E_{g,pd}$  from max. rate) samples; (c) temperature dependence of Urbach energy.

as explained by the Varshni model,<sup>15</sup> Bose-Einstein model<sup>16</sup> and Pässler model<sup>17</sup> or due to thermal lattice expansion.<sup>18,19</sup> Furthermore, Figure 1(a) shows a variation in the slope of the transmission spectra, which indicates a change in band tailing with temperature. From the spectra presented in Figure 1(a) the absorption coefficient  $\alpha$  was extracted by inverse Beer-Lambert relation for more detailed evaluation of the band gap behavior, i.e.  $\alpha = -\ln(T)/d$ , where  $T$  represents the transmission and  $d$  the thickness of the film. The extracted absorption coefficients are then used for evaluation of the band gap and the behavior of the Urbach tails.

The band gap evaluation was performed by fitting the spectra with a square root function<sup>14</sup> in the energy range above 1.15 eV, which is sufficiently above the band gap and not influenced by tail states. Other methods for evaluation of the band gap were additionally tested but gave no significant difference in the results, indicating that the presented results can be considered as robust.

The results for all applied cooling rates as well as for the spectra recorded at room temperature for the ‘as-prepared’ and ‘disordered’ samples are plotted as a function of temperature in Figure 1(b). For temperatures higher than  $\approx 210$  °C the band gap energy shows a linear behavior with the same slope for all cooling rates. For temperatures lower than  $\approx 210$  °C the band gap energies depend on the cooling rate, i.e. for higher cooling rates the band gap increases less with decreasing temperature than for lower cooling rates. For temperatures below  $\approx 140$  °C the band gap values differ strongly for the different cooling rates, but change only slightly with further cooling down, and show again a similar slope for all cooling rates for this temperature regime.

To clarify the temperature dependent behavior of the band gap, Figure 1(b) shows  $\Delta E_g$  ( $E_{g,po} - E_{g,pd}$ ) values, which were calculated by subtracting the band gap energies of the maximal cooling rate (which leads finally to a preferentially disordered sample state “pd”) from the 0.5 °C/min rate (which ends up in a preferentially ordered sample state “po”). In the temperature regime  $> 210$  °C the  $\Delta E_g$  values stay constant with temperature. This means, that the CZTSe crystal is completely disordered and the temperature dependence of the band gap is mainly due to electron-phonon interaction or thermal lattice expansion and is the same for different cooling rates. For temperatures  $< 210$  °C  $\Delta E_g$  increases strongly, originating from the different degrees of order which are being established for the two different cooling rates, i.e. during cooling with 0.5 °C/min a higher degree of order can be reached than during cooling with maximal rate. From this behavior of  $\Delta E_g$  we determine the critical temperature  $T_c$  for CZTSe to be  $(210 \pm 5)$  °C, which is the onset temperature for the disorder-order transition. This particular result is in agreement with the results published by Rey *et al.*,<sup>10</sup> however in this study we were able to observe the phase transition in-situ, which allows us not only to specify the starting point of the phase transition but additionally to specify the temperature range between 210 and 140 °C as a control temperature range. The choice of the cooling ramp within this control range determines the resulting degree of order. As the ordering kinetics below this range is dramatically reduced  $\Delta E_g$  shows a constant behavior again for temperatures below 140 °C, i.e. the temperature dependent change in band gap is similar for the two cooling rates.

The band gap behavior in this temperature regime is again mainly determined by electron-phonon interaction or thermal lattice contraction and is comparable for samples with higher and lower degree of order. As the ordering kinetics at lower temperature is slowed down significantly, it does not show any effect at the time scales of these two cooling rates. Consequently we can conclude that the degree of order which is established within the range of 210 to 140 °C is conserved below 140 °C.

Furthermore, we are able to extract tailing properties from the sub gap behavior of the absorption coefficients.<sup>20</sup> The temperature dependence of the Urbach tails is plotted in Figure 1(c). We show the Urbach energy as a function of temperature, normalized by the Urbach energy at room temperature. The plotted values show only a slight temperature dependence for the range from room temperature to 180 °C. Between 180 and 250 °C we find a step like behavior. This can be explained by a decreasing Urbach energy for lower temperatures<sup>21,22</sup> combined with the effect of ordering during cooling down, which may lead to a reduced Urbach energy when compared to the fully disordered state at  $\approx 250$  °C. However, there is no clear indication from literature that the degree of order at room temperature has an impact on the Urbach energy.<sup>2</sup> For reliable extraction of the absolute values of the Urbach energy we have performed additional ex-situ transmission and reflection measurements with an integrating sphere. We find Urbach energies of  $70 \pm 5$  meV for both preferentially ordered and disordered samples.

In the inset in Figure 2 transmission spectra are presented which were recorded subsequently during annealing at 122 °C for 15 h. The ‘in-situ’ sample was used for this experiment after a disordering step as described above. The shift of the absorption edge with time represents the change of the band gap due to the ordering process in the Cu-Zn planes of the CZTSe crystal during this temperature treatment. Figure 2 displays the time evolution of the band gap energies extracted from the transmission spectra. This evolution exhibits very slow kinetics for the phase transition from disordered to ordered CZTSe. Note, that by cooling down to 30 °C after approximately 15 h the band gap increases additionally. This is related to the temperature dependence of the band gap of semiconductors due to electron-phonon interaction and lattice contraction, which was already discussed above. The band gap value extracted from the sample ‘in-situ’ at the end of the 15 h temperature treatment reached 0.979 eV. This was the highest value, meaning the highest degree of order, which was observed during this study. By longer annealing at lower temperatures the degree of order might be even more increased.<sup>5,13,23</sup> However, such long post deposition treatments are not suitable in fabrication processes, as already pointed out in other studies.<sup>9</sup> Therefore we combine the findings from our in-situ transmission experiments, to propose a cooling procedure, which ought to take advantage of the found control temperature range between 210 and 140 °C. Hence, it is sufficient to focus on the cooling rate between 210 °C and 140 °C for processing preferentially ordered CZTSe films. Outside of this range higher cooling rates can be applied with no noticeable influence on the degree of order. This is particularly relevant for higher temperatures around usual process temperatures (typically around 500 to 550 °C), as slow cooling rates in this range may cause decomposition of the CZTSe phase. In conclusion we suggest a fast cooling between process temperature and the critical temperature  $T_c$ , followed by a slow cooling in the discussed control temperature range of 210 to 140 °C, and a final fast cooling down to room temperature, to get preferentially ordered CZTSe samples while maintaining an acceptable duration for the cool down step after high temperature processing.

Figure 3(a) displays Raman spectra of the samples ‘as-prepared’, ‘disordered’ and ‘in-situ’ after the different temperature treatments. The A-modes in the Raman spectra show a peak broadening, decreasing intensity, and a shift to lower wavenumbers with increasing degree of disorder, which is in agreement with the results of Rey *et al.*<sup>10</sup> Furthermore for the disordered state two A-modes at around 170 and 194  $\text{cm}^{-1}$  can be identified, whereas in the spectra for the preferentially ordered state (after 15 h annealing and after cooling with 0.5 °C/min) a shoulder at approx. 168  $\text{cm}^{-1}$  appears, which implies that three A-modes are present as expected for preferentially ordered CZTSe. The intensity ratio of the modes in the range between 210 and 255  $\text{cm}^{-1}$  (inset in Figure 3(a)) varies with the degree of order in the sample. We define two ratios of Raman intensities: (i) the ratio of the maxima of the A modes  $Q_{\text{CZTSe}} = I(\sim 172)/I(\sim 195)$  and (ii) the ratio  $Q^*_{\text{CZTSe}} = I(233)/I(220)$  of the Raman modes at around 233  $\text{cm}^{-1}$  (sum of interval 233  $\pm$  4  $\text{cm}^{-1}$ ) and at around 220  $\text{cm}^{-1}$  (sum of interval 220  $\pm$  4  $\text{cm}^{-1}$ ). Figure 3(b) shows the values of these two ratios plotted as a function of the band gap,

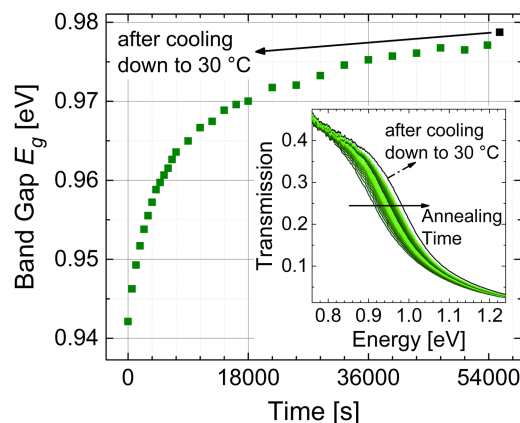


FIG. 2. Extracted band gap energy of CZTSe at 122 °C during 15 h annealing time and at 30 °C after cooling, inset: In-situ transmission spectra recorded during this experiment.

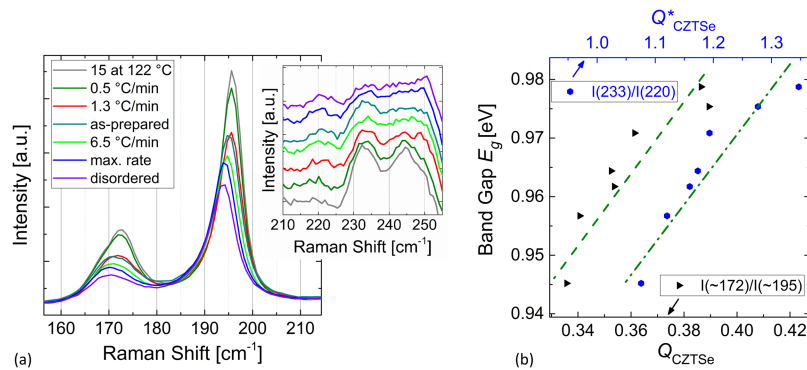


FIG. 3. (a) Raman spectra recorded at room temperature on samples ‘as-prepared’, ‘disordered’ and ‘in-situ’ after different temperature treatments, inset: zoomed in view for the spectral region between 210 and 255 cm<sup>-1</sup> (spectra plotted with offset for better viewing); (b) relation between band gap energies (i.e. different degree of order) and the Raman mode intensity ratios  $Q_{\text{CZTSe}}$  and  $Q^*_{\text{CZTSe}}$  (green dashed lines are guides to the eye).

which is connected to the degree of order. Both ratios exhibit a clear correlation with the extracted band gaps. Therefore we conclude that Raman analysis, as a fast and non-destructive method, can be used as a tool to determine a secondary order parameter for CZTSe, as it was already shown for CZTS.<sup>8,9</sup>

To conclude, we investigated the order-disorder transition in CZTSe during heat treatment and cooling procedures by in-situ transmission spectroscopy. By determination of the band gap energies depending on temperature and cooling rates, we found the critical temperature of this transition to be  $T_c = (210 \pm 5)^\circ\text{C}$ . Further, a control temperature range between 210 and 140 °C was found, which allows for obtaining preferentially ordered films during cool down. During an annealing treatment at a constant temperature below  $T_c$  we observed very slow kinetics for the ordering process. This implies that for achieving highly ordered CZTSe thin films long post deposition treatments would be necessary, which are not realistic for usual fabrication processes. Therefore we suggest a defined cooling procedure by considering the presented control temperature range, which leads to a compromise between process duration and degree of order in CZTSe samples.

Our results show a change of the Urbach energy in the region of the critical temperature, indicating an influence of the degree of order on the tailing properties of the band gap. Nevertheless, at room temperature no difference of the Urbach energy for different degrees of order was found.

Furthermore, we showed that Raman spectroscopy can be applied as a fast method for determining the degree of order in CZTSe thin films by using intensity ratios of common Raman modes as a secondary order parameter.

## ACKNOWLEDGMENTS

The authors gratefully acknowledge funding from EWE AG Oldenburg – Germany, funding from German ministry of Education and Science (BMBF, contract No 03SF0530A) and funding from Fond National de la Recherche (FNR, project KITS2).

Jörg Ohland, Dennis Wilken, Dirk Otteken, Thomas Madena, Matthias Macke and Holger Koch (Univ. Oldenburg) are acknowledged for technical support and fruitful discussion.

<sup>1</sup> S. W. Wang, M. T. Winkler, O. Gunawan, T. Gokmen, T. K. Todorov, Y. Zhu, and D. B. Mitzi, *Adv. Energy Mater.* **4**, 1301465 (2014).

<sup>2</sup> S. Bourdais, C. Choné, B. Delatouche, A. Jacob, G. Larramona, C. Moisan, A. Lafond, F. Donatini, G. Rey, S. Siebentritt, A. Walsh, and G. Dennler, *Adv. Energy Mater.*, 1502276 (2016).

<sup>3</sup> G. Rey, T. P. Weiss, J. Sendler, A. Finger, C. Spindler, F. Werner, M. Melchiorre, M. Hála, M. Guennou, and S. Siebentritt, *Sol. Energy Mater. Sol. Cells* **151**, 131 (2016).

<sup>4</sup> C. Krämer, C. Huber, T. Schnabel, C. Zimmermann, M. Lang, E. Ahlswede, H. Kalt, and M. Hetterich, Proc. 42nd IEEE Photovoltaic Specialist Conference (2015).

<sup>5</sup> J. J. S. Scragg, J. K. Larson, M. Kumar, C. Persson, J. Sendler, S. Siebentritt, and C. Platzer Björkmann, *Phys. Status Solidi B* **253**, 247 (2016).

<sup>6</sup> S. Schorr, *Sol. Energy Mater. Sol. Cells* **95**, 1482 (2011).

- <sup>7</sup> L. Choubrac, M. Paris, A. Lafond, C. Guillot-Deudon, X. Rocquefelte, and S. Jobic, *Phys. Chem. Chem. Phys.* **15**, 10722 (2013).
- <sup>8</sup> J. J. S. Scragg, L. Choubrac, A. Lafond, T. Ericson, and C. Platzer-Björkmann, *Appl. Phys. Lett.* **104**, 041911 (2014).
- <sup>9</sup> K. Rudisch, Y. Ren, C. Platzer-Björkmann, and J. Scragg, *Appl. Phys. Lett.* **108**, 231902 (2016).
- <sup>10</sup> G. Rey, A. Redinger, J. Sendler, T. P. Weiss, M. Thevenin, M. Guennou, B. El Adib, and S. Siebentritt, *Appl. Phys. Lett.* **105**, 112106 (2014).
- <sup>11</sup> G.H. Vineyard, *Phys. Rev.* **102**, 981 (1956).
- <sup>12</sup> D. M. Többens, G. Gurieva, S. Levchenko, T. Unold, and S. Schorr, *Phys. Status Solidi B* **1–8** (2016).
- <sup>13</sup> C. Krämer, C. Huber, C. Zimmermann, M. Lang, T. Schnabel, T. Abzieher, E. Ahlswede, H. Kalt, and M. Hetterich, *Appl. Phys. Lett.* **105**, 262104 (2014).
- <sup>14</sup> A. Redinger, J. Sendler, R. Djemour, T. P. Weiss, G. Rey, and S. Siebentritt, *IEEE J. Photovolt.* **5**, 641 (2015).
- <sup>15</sup> Y. P. Varshni, *Physica* **34**, 149 (1967).
- <sup>16</sup> P. Lautenschlager, M. Garriga, S. Logothetidis, and M. Cardona, *Phys. Rev. B* **35**, 9174 (1987).
- <sup>17</sup> R. Pässler, *Phys. Status Solidi B* **200**, 155 (1997).
- <sup>18</sup> A. Manoogian and A. Leclerc, *Can. J. Phys.* **57**, 1766 (1979).
- <sup>19</sup> C. Rincón, S. M. Wasim, G. Marin, and I. Molina, *J. Appl. Phys.* **93**, 780 (2003).
- <sup>20</sup> F. Urbach, *Phys. Rev.* **92**, 1324 (1953).
- <sup>21</sup> G. D. Cody, T. Tiedje, B. Abeles, B. Brooks, and Y. Goldstein, *Phys. Rev. Lett.* **47**, 1480 (1981).
- <sup>22</sup> Z. Yang, K. P. Homewood, M. S. Finney, M. A. Harry, and K. J. Reeson, *J. Appl. Phys.* **78**, 1958 (1995).
- <sup>23</sup> M. Valentini, C. Malerba, F. Menchini, D. Tedeschi, A. Plimeni, M. Capizzi, and A. Mittiga, *Appl. Phys. Lett.* **108**, 211909 (2016).

## In-situ investigation of the order-disorder transition in $\text{Cu}_2\text{ZnSnSe}_4$ by optical transmission spectroscopy

Christiane Stroth, Mohamed H. Sayed, Janet Neerken, Ulf Mikolajczak, Germain Rey, Jürgen Parisi, and Levent Gütaý

Citation: *AIP Advances* **7**, 025303 (2017); doi: 10.1063/1.4976619

View online: <http://dx.doi.org/10.1063/1.4976619>

View Table of Contents: <http://aip.scitation.org/toc/adv/7/2>

Published by the [American Institute of Physics](#)

---

### Articles you may be interested in

[Modification of defects and potential fluctuations in slow-cooled and quenched  \$\text{Cu}\_2\text{ZnSnSe}\_4\$  single crystals](#)

*Journal of Applied Physics* **121**, 065704 (2017); 10.1063/1.4975483

[Controlling metastable native point-defect populations in  \$\text{Cu}\(\text{In,Ga}\)\text{Se}\_2\$  and  \$\text{Cu}\_2\text{ZnSnSe}\_4\$  materials and solar cells through voltage-bias annealing](#)

*Journal of Applied Physics* **121**, 043102 (2017); 10.1063/1.4973959

[Discrepancy between integral and local composition in off-stoichiometric  \$\text{Cu}\_2\text{ZnSnSe}\_4\$  kesterites: A pitfall for classification](#)

*Applied Physics Letters* **110**, 043901 (2017); 10.1063/1.4974819

[Interface band gap narrowing behind open circuit voltage losses in  \$\text{Cu}\_2\text{ZnSnS}\_4\$  solar cells](#)

*Applied Physics Letters* **110**, 083903 (2017); 10.1063/1.4976830

[Structural transitions of ordered kesterite-type  \$\text{Cu}\_2\text{ZnSnS}\_4\$  under pressure](#)

*Applied Physics Letters* **110**, 041905 (2017); 10.1063/1.4974941

[Compositional dependence of charge carrier transport in kesterite  \$\text{Cu}\_2\text{ZnSnS}\_4\$  solar cells](#)

*Journal of Applied Physics* **120**, 225703 (2016); 10.1063/1.4971179

---

# HAVE YOU HEARD?

Employers hiring scientists and engineers trust

**PHYSICS TODAY | JOBS**

[www.physicstoday.org/jobs](http://www.physicstoday.org/jobs)

